

## Effects of DC bias voltages on the RF-excited plasma–tissue interaction

This content has been downloaded from IOPscience. Please scroll down to see the full text.

2016 J. Phys. D: Appl. Phys. 49 415201

(<http://iopscience.iop.org/0022-3727/49/41/415201>)

View [the table of contents for this issue](#), or go to the [journal homepage](#) for more

Download details:

IP Address: 202.117.25.61

This content was downloaded on 14/09/2016 at 00:34

Please note that [terms and conditions apply](#).

# Effects of DC bias voltages on the RF-excited plasma–tissue interaction

Aijun Yang<sup>1</sup>, Dingxin Liu<sup>1</sup>, Xiaohua Wang<sup>1</sup>, Jiafeng Li<sup>1</sup>, Chen Chen<sup>1</sup>, Mingzhe Rong<sup>1</sup> and Michael G Kong<sup>1,2,3</sup>

<sup>1</sup> State Key Laboratory of Electrical Insulation and Power Equipment, Centre for Plasma Biomedicine, Xi'an Jiaotong University, Xi'an 710049, People's Republic of China

<sup>2</sup> Frank Reidy Center for Bioelectronics, Old Dominion University, Norfolk, VA 23508, USA

<sup>3</sup> Department of Electrical and Computer Engineering, Old Dominion University, Norfolk, VA 23529, USA

E-mail: [liudingxin@mail.xjtu.edu.cn](mailto:liudingxin@mail.xjtu.edu.cn) and [mglin5g@gmail.com](mailto:mglin5g@gmail.com)

Received 3 May 2016, revised 18 August 2016

Accepted for publication 19 August 2016

Published 13 September 2016



## Abstract

We present in this study how DC bias voltage impacts on the fluxes of reactive species on the skin tissue by means of a plasma–tissue interaction model. The DC bias voltage inputs less than 2% of the total discharge power, and hence it has little influence on the whole plasma characteristics including the volume-averaged densities of reactive species and the heating effect. However, it pushes the plasma bulk towards the skin surface, which significantly changes the local plasma characteristics in the vicinity of the skin surface, and in consequence remarkably enhances the flux densities of reactive species on the skin tissue. With the consideration of plasma dosage and heat damage on the skin tissue, DC bias voltage is a better approach compared with the common approach of increasing the plasma power. Since the DC voltage is easy to apply on the human body, it is a promising approach for use in clinical applications.

Keywords: DC bias voltage, flux density, reactive species, plasma medicine

(Some figures may appear in colour only in the online journal)

## 1. Introduction

Recent years have witnessed a significant research interest in the treatment of living materials such as human skin with cold atmospheric-pressure plasmas (CAPs) [1, 2]. Although the mechanism of CAPs' biological effects is far from being understood, it is widely accepted that the plasma-generated reactive species such as O and OH play a dominant role [1, 3]. Therefore, many research works have been reported on the quantification and/or control of the volume densities of the reactive species in the last decade [4]. The volume density reflects the yield of a species, but it may have a different variation trend with the flux density acting on the living materials. Taking O\* in a radio-frequency (RF) discharge for example, we have previously reported that the flux density and the volume-averaged density had much different dependences on the discharge gap width, the driving frequency, the feeding gas composition, and so on [5–7]. The time integrals of the

flux densities (the fluences) of reactive species on the treated sample represent the plasma dosage, which has been reported to be sensitive for achieving a desired biomedical effect [8, 9]. Therefore, it is of significance to precisely control and optimize the flux densities rather than the volume densities of the reactive species for biomedical applications.

One important aspect for optimizing the flux density is to enhance its energy efficiency. This is not just for energy conservation, it is more important to achieve sufficient plasma dosage for the desired biomedical effect with minimal heat damage and treatment time. The heat damage to the living tissue can be estimated by an empirical formula [10, 11]

$$\Omega = \int_0^t A \exp(-E_a/RT_n) dt \quad (1)$$

where  $\Omega$  is the heat damage index,  $A$  is a frequency factor that depends on molecular structure,  $E_a$  is the activation energy,  $R$  is the general gas constant, and  $T_n$  is the temperature at a

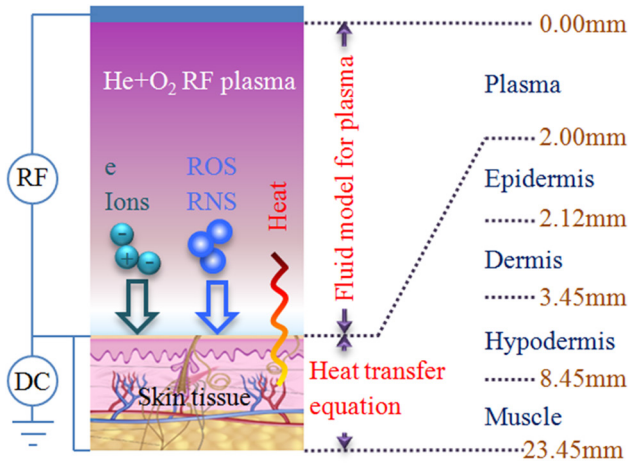


Figure 1. Diagram of the plasma–tissue interaction model.

point in the tissue. The heat damage is accumulated with the treatment time, and it will be irreversible when  $\Omega \geq 1$ . Various approaches have been reported for enhancing the flux densities of reactive species, but many of them have the drawback of remarkably increasing the heating effect simultaneously [1, 12], and hence the plasma dosage for continuous treatment may not increase because the endurable treatment time is reduced.

Is there any novel method to enhance the flux densities of reactive species without significantly increasing the heating effect? From the researches on low-pressure plasmas, a small DC bias voltage is capable of enhancing the ion flux density on the treated sample and hence benefits applications such as film deposition and etching [13–15]. With the DC bias voltage, it is also possible to enhance the flux densities of reactive species in CAPs, but to our knowledge this has never been reported so far. The reports for DC bias voltages used in CAPs are just for improving the plasma stability, the surface charging performance as well as the airflow control [16–18]. This motivates us to make a tentative study on the correlation between small DC bias voltages and the flux densities of reactive species on the living materials.

## 2. Description of the computational model

An integration model for the interaction of RF plasmas and human skin has been reported by our group [11], and it is used here with a little modification. The structure of the model is illustrated in figure 1, in which the discharge gap (plasma region) is 2 mm, the thickness of skin tissue is 21.45 mm, and the feeding gas for discharge is He + 0.5%O<sub>2</sub>. The thicknesses of the skin tissue and its sub-layers are referred from [19]. A RF source with frequency of 13.56 MHz is applied on the discharge gap, and a DC source is applied on the skin tissue (the whole tissue has the same potential). The DC voltage biases the cycle symmetry of the discharge voltage. Considering the safety requirements for clinical applications, the DC voltage varies from 0 to 80V according to IEC/TS 61201-2007. The total input power of the RF and DC sources is kept constant to be 2 W cm<sup>-3</sup>.

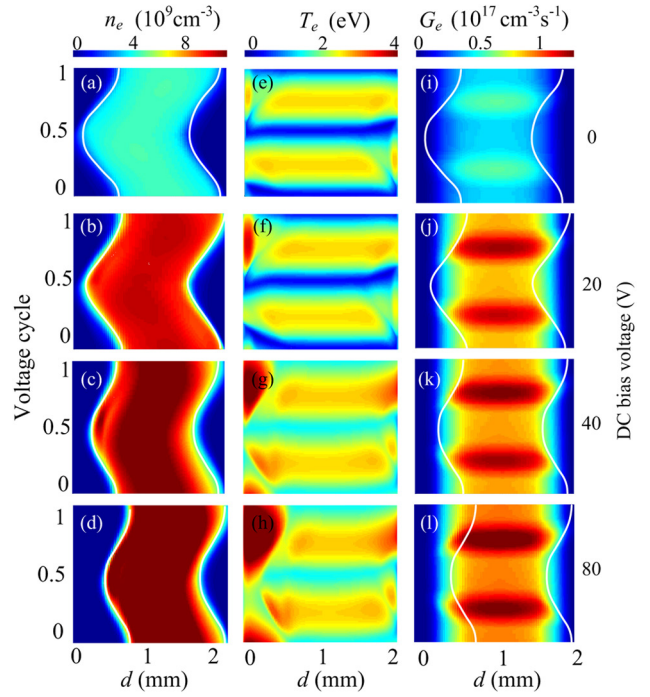


Figure 2. Spatio-temporal profiles of (a)–(d) electron density ( $n_e$ ), (e)–(h) electron temperature ( $T_e$ ) and (i)–(l) electron generation rate ( $G_e$ ) in the plasma region for different DC bias voltages.  $d$  is the distance from the electrode which is opposite to the skin as shown in figure 1. The white curves represent the sheath boundaries.

According to [20], we take into account 17 species: electrons ( $e$ ), positive ions ( $O_2^+$ ,  $O_4^+$ ), negative ions ( $O^-$ ,  $O_2^-$ ,  $O_3^-$ ), electronic excited species ( $He^*$ ,  $He_2^*$ ,  $O(^1D)$ ,  $O(^1S)$ ,  $O_2(a^1\Delta_g)$  and  $O_2(b^1\Sigma_g^+)$ ), vibrational excited species ( $O_{2v}$ ,  $v = 1-4$ ) and ground state neutrals ( $He$ ,  $O_2$ ,  $O$ , and  $O_3$ ). The 60 reactions considered in the model are also obtained from [20]. For the plasma area, the drift-diffusion equation for each species, the electron energy equation, Poisson’s equation and the gas heating equation are considered. The first three governing equations are similar to publications by other research groups [21, 22] and are detailed in our previous publications [11, 20]. The gas heating equation is described by

$$\rho_g c_g \frac{\partial T_g}{\partial t} + \nabla \cdot (-k_g \nabla T_g) = Q \quad (2)$$

where  $\rho_g$ ,  $c_g$ ,  $k_g$ , and  $T_g$  are the density, specific heat capacity, thermal conductivity and temperature of the gas, respectively.  $Q$  is the heating due to momentum transfer between electrons and species  $i$  and ion Joule heating and given by

$$Q = \sum_i \frac{m_e}{m_i} K_B R_{el,i} (T_e - T_g) + \mathbf{J}_{ion} \cdot \mathbf{E} \quad (3)$$

where  $m_e$  and  $T_e$  are the mass and temperature of electrons;  $m_i$  and  $R_{el,i}$  are the mass of species  $i$  and the momentum transfer rate with electrons;  $K_B$ ,  $\mathbf{J}_{ion}$  and  $\mathbf{E}$  are the Boltzmann constant, ion current and electric field.

In this study, the DC bias voltage is applied on the tissue surface, as shown in figure 1. In practice, this corresponds to the fact that a copper wire mesh (a few micrometers in thickness) is put on the surface of a treated sample and the DC bias voltage

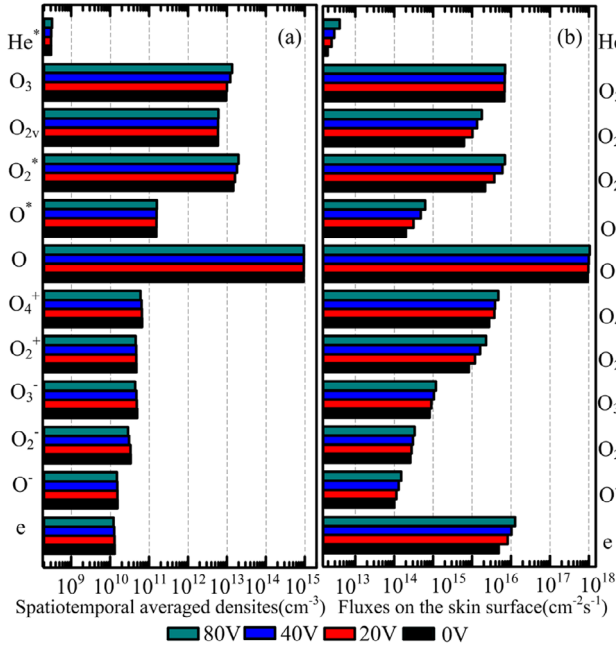


**Figure 3.** (a) Spatiotemporal-averaged volume densities and (b) cycle-averaged flux densities of reactive species for different DC bias voltages around plasma treatment time of 100 s.

is applied on the mesh. The reactive species can deliver to the skin surface through the mesh, but no current can flow through the skin tissue since the whole tissue has the same potential. Therefore, Poisson’s equation is not solved for the tissue area and only the Pennes heat transfer equation is considered:

$$\rho_s c_s \frac{\partial T_s}{\partial t} = k_s \nabla^2 T_b + \varpi_b \rho_b c_b (T_b - T_s) + q_{met} \quad (4)$$

where  $\rho_s$ ,  $c_s$ ,  $k_s$ , and  $T_s$  are the density, specific heat capacity, thermal conductivity and temperature of the skin tissue, respectively;  $\varpi_b$ ,  $\rho_b$ ,  $c_b$  and  $T_b$  are the perfusion rate, density, specific heat capacity and temperature of the blood, respectively; the second term on the right hand side is the net heat resulted from blood perfusion;  $q_{met}$  is heat generated by metabolism. Thermal parameters of the skin tissue and blood can be obtained from [11]. It is noted that the heat transfer equations in the plasma and tissue areas are of the same form, and can be solved continuously from the plasma area to the tissue area. The temperature of the electrode is fixed to be 300 K, and the temperature in the underside of the skin tissue is fixed to be 310 K (37 °C).

### 3. Results and discussions

According to the simulation, the spatiotemporal distributions of electron density, electron temperature and electron generation rate in the plasma region are plotted in figure 2, for the DC bias voltages of 0, 20, 40 and 80V. The white curves in the sub-figures represent the sheath boundaries determined by  $n_- = 0.3 n_+$ , in which  $n_+$  and  $n_-$  are the densities of positive and negative charged species, respectively [7, 23]. To facilitate the following discussions, the plasma region is divided into three sub-regions, namely PS1 for the plasma sheath opposite

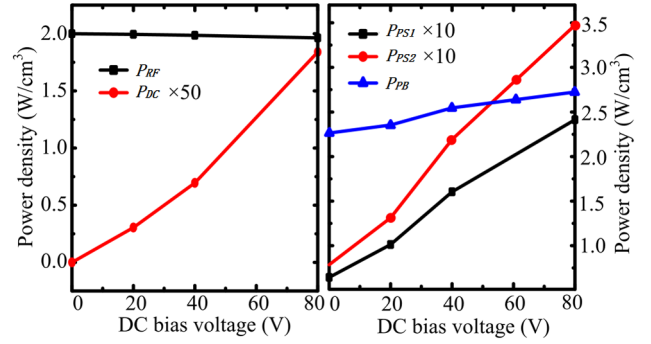


**Figure 4.** (a) The power supplied by RF source ( $P_{RF}$ ) and DC source ( $P_{DC}$ ), as well as (b) the dissipated power densities in PS1 ( $P_{PS1}$ ), PB ( $P_{PB}$ ) and PS2 ( $P_{PS2}$ ) as a function of the DC bias voltage.

to the skin, PB for the quasi-neutral plasma bulk, and PS2 for the plasma sheath adjacent to the skin.

As shown in figures 2(a)–(d), the electrons oscillate between the electrode and the skin, and PB has its width nearly constant during each voltage cycle. With DC bias voltage increasing from 0 to 80V, the width of PB decreases slightly from 1.56 to 1.33 mm, the maximum width of PS1 increases from 0.33 to 0.70 mm, and the maximum width of PS2 decreases from 0.42 to 0.36 mm. The electron density has its peak increase from  $1.97 \times 10^{10}$  to  $2.35 \times 10^{10} \text{ cm}^{-3}$ , but in average it is nearly unperturbed. The DC bias voltages push the plasma bulk towards the skin tissue, and in consequence change the sheath dynamics to a large extent. For example, the maximal electron temperature in PS1 increases from 2.70 to 4.66 eV, and in PS2 it increases from 2.68 to 3.61 eV (see figures 2(e)–(h)). Moreover, the average electron density in PS2 increases from  $2.29 \times 10^8$  to  $9.53 \times 10^8 \text{ cm}^{-3}$  (not shown clearly in figure 2). The increases of both electron density and electron temperature in PS2 will certainly result in higher production rates of reactive species in the vicinity of the skin tissue, which consequently enhance the flux densities of reactive species as will be discussed below. Regarding the electron generation rate, it is dominant in PB for all the cases (see figures 2(i)–(l)), suggesting that the plasmas are in  $\alpha$  mode. The electron generation rate in PB increases slightly with DC bias voltage to compensate the correspondingly increasing boundary loss of charged species as shown in figure 3.

The influences of DC bias voltage on the volume densities and flux densities of reactive species are shown in figure 3, in which  $O_2^*$  represents  $O_2(a^1\Delta_g)$  and  $O_2(b^1\Sigma_g^+)$ ,  $O^*$  represents  $O(^1D)$  and  $O(^1S)$ , and  $O_{2v}$  represents the vibrational excited  $O_2$ . In general, higher volume density correlates to higher flux density. For example, the ground state O has the maximal volume density as well as the flux density, while for the helium metastable both densities are minimal due to its strong reduction via Penning ionization [24, 25]. However, this is not always true for charged species, for example the volume density of  $O_3^-$  is higher than that of  $O_2^+$ , but the flux density of  $O_3^-$  is comparatively less by around one order of magnitude. This is due to the ambipolar field which traps the anions in the centre part of the plasma [5–7].

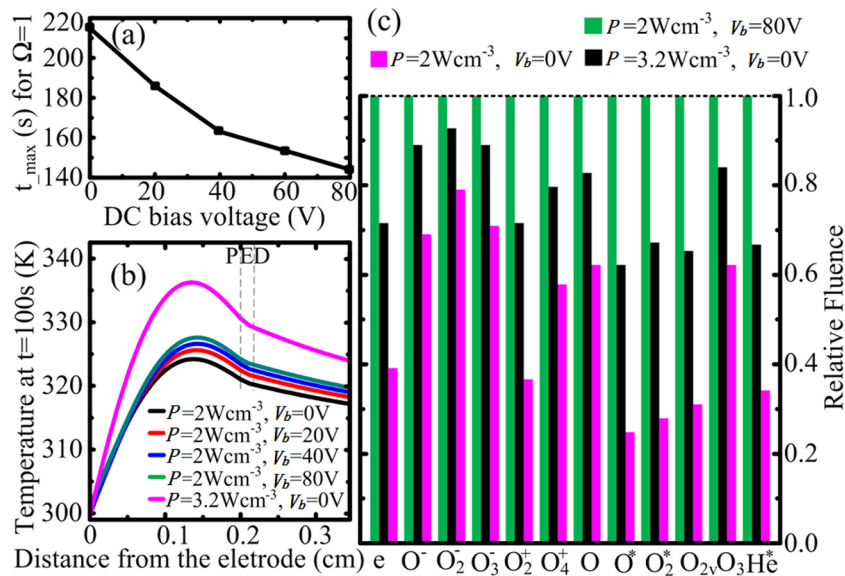


**Figure 5.** (a) Maximum time of continuous treatment up to  $\Omega = 1$  for different DC bias voltages with constant total power density of  $2\text{W cm}^{-3}$ ; (b) temperature distributions in plasma (P), epidermis (E) and dermis (D) at the treatment of 100 s. (c) Relative fluences of reactive species on the skin tissue for different discharge conditions, of which the fluences are normalized to those for the condition of power density =  $2\text{W cm}^{-3}$  and DC bias voltage = 80 V.

The flux densities on the skin tissue of all the reactive species increase with DC bias voltage, but the volume densities have different variation trends for different species (see figure 3). It is noted that we also investigated the impact of negative DC bias voltage on the fluxes of reactive species and found that negative DC bias voltage significantly decreased the fluxes of reactive species, especially for electron and negative ions. Therefore, negative DC bias voltage is not discussed in detail. For the flux density,  $O_2^*$  has the maximal increment of more than 260%, while  $O_3$  has the minimal increment of only  $\sim 10\%$ . For the volume density,  $O_3$  increases mostly by  $\sim 40\%$ , but  $O_2^-$  decreases largest by  $\sim 15\%$ . With DC bias voltage increasing from 0 to 80 V, the average change (absolute value) for the flux densities of all the species is 107.6%, while for the volume densities it is just 11.9%, less by nearly one order of magnitude. Both the negative and positive charged species have their fluxes increasing with DC bias voltage, suggesting that the electric field force should not be the main reason for their increments. The reactive species have short lifetimes in CAPs and hence their movement distances during lifetime are typically less than  $200\ \mu\text{m}$  [5–7]. Therefore, the reactive species acting on the skin tissue should be mainly supplied by the local plasma region near to the skin, which is roughly the PS2. As discussed above, both the electron density and electron temperature in PS2 increase with DC bias voltage, leading to higher densities of reactive species in such a local region, and consequently enhance their fluxes on the skin tissue. This may also explain why the influence of DC bias voltage on the flux densities is generally much more pronounced than that on the volume densities.

Why do the electron density and electron temperature increase in PS2 with the DC bias voltage despite of the invariable total input power? In order to elucidate the underlying mechanism, we plotted in figure 4 the power supply and dissipation in the plasma regions of PS1, PB and PS2. As shown in figure 4(a), the power density supplied by the RF source ( $P_{\text{RF}}$ )

decreases but the power density supplied by the DC source ( $P_{\text{DC}}$ ) increases with the increasing DC voltage. In contrast to RF power density, it is interesting that the RF voltage increases from  $\sim 233$  to  $\sim 245$  V. The DC power density is much lower than the RF power density, which is at most  $\sim 0.036\text{W cm}^{-3}$  when DC voltage is equal to 80 V. However, it dramatically changes the power dissipations in the sheath regions of the plasma (see figure 4(b)).

As shown in figure 4(b), the dissipated power densities in the plasma regions of PS1, PB and PS2 keep increasing with DC bias voltage. The increments are  $\sim 1.2$  in PB,  $\sim 6.4$  in PS1, and  $\sim 9.2$  in PS2 with DC bias voltage increasing from 0 to 80 V. Although the power densities in all three regions of the plasma increase, it is noted that the average power density remains invariable because PB narrows down (see figure 2) and the power density in PB is much larger than those in PS1 and PS2. Since the dissipated power density in PS2 increases by nearly one order of magnitude, the electron density and electron temperature increase there accordingly (see figure 2). This yields more reactive species in the vicinity of the skin tissue, and finally enhances the flux densities. The DC bias voltage increases the flux densities of reactive species by at most 2.6 fold (for  $O_2^*$  as shown in figure 3) with less than 2% of the total power injection, so it is an energy-efficient approach for enhancing the flux densities of reactive species.

Besides the energy efficiency, what is more important for clinical applications is to generate a plasma with large fluxes of reactive species and near body temperature. Continuously heating may lead to irreversible damage of the living tissues as can be estimated by formula (1) with  $\Omega \geq 1$ , which needs to be avoided for clinical applications [10]. In this regard, the maximal fluences of reactive species for continuous plasma treatment should be restricted by the criterion of  $\Omega = 1$ , which depends on both the plasma–tissue heating intensity and the treatment time. In order to demonstrate that DC bias

voltage is an efficient approach to enhance the plasma dosage on living tissues, the maximal time of continuous treatment (corresponding to  $\Omega = 1$ ), the temperature distribution in the skin tissue at a moment, and the maximal fluences (relative values) of reactive species on the skin tissue are compared for the plasmas with and without DC bias voltages, as well as the non-biased plasma with higher power density of  $3.2 \text{ W cm}^{-3}$ , as are shown in figure 5. When the power density is  $3.2 \text{ W cm}^{-3}$ , the flux of electrons is the same to the plasma with power density of  $2 \text{ W cm}^{-3}$  and DC bias voltage of 80V.

As shown in figure 5(a), it is interesting that the maximal treatment time decreases by nearly one third from 215 to 144s with DC bias voltage increasing from 0 to 80V, although the total power density of the plasmas is invariable. This is because more power is dissipated in the local plasma region near the tissue (see figure 4(b)), and hence the heat flux on the tissue is enhanced. As shown in figure 5(b), the temperature in the skin tissue increases with the DC bias voltage for the same treatment time of 100s. One common approach for enhancing the flux densities of reactive species is to increase the plasma power density, but the heating effect is enhanced correspondingly, which will in turn decrease the maximal time of continuous plasma treatment. For the non-biased RF plasma with power density of  $3.2 \text{ W cm}^{-3}$ , the temperature in the skin tissue at the treatment time of 100s is much higher (see figure 5(b)), and correspondingly the maximal time for continuous treatment is reduced to just 90s.

As shown in figure 5(c), the DC bias voltage increases the maximal fluences of all the reactive species significantly for continuous plasma treatment. Compared with the common approach for optimizing the fluences of reactive species by increasing the plasma power density, the increments of fluences by DC bias voltage are more pronounced for all the reactive species. The most increment happens for  $\text{O}^*$  of  $\sim 4.5$  fold with  $V_b = 80 \text{ V}$ , while it is just  $\sim 2.7$  fold by increasing the plasma power (see figure 5(c)). Therefore, the DC bias voltage is a novel approach to enhance the plasma dosage on living tissues.

#### 4. Conclusions

In summation, the DC bias voltage introduces little power to the RF plasma and has little influence on the whole plasma characteristics including the volume densities of reactive species and the heating effect, but it significantly changes the local plasma characteristics in the vicinity of the skin surface, which in consequence remarkably enhances the flux densities of reactive species on the skin tissue while restricting the increase of heating effect. This makes the DC bias voltage a better approach for optimizing the plasma dosage on living materials compared with the common approaches such as increasing the plasma power. The DC voltage is easy to apply on the human body, and it is a promising approach for use in clinical applications.

#### Acknowledgments

This work was supported by the National Science Foundation of China (Grant No. 51521065), the China Postdoctoral Science Foundation (No. 2015M572558) and the State Key Laboratory of Electrical Insulation and Power Equipment (No. EIPE16307).

#### References

- [1] Kong M G, Kroesen G, Morfill G, Nosenko T, Shimizu T, Van Dijk J and Zimmermann J L 2009 *New J. Phys.* **11** 115012
- [2] Fridman G, Friedman G, Gutsol A, Shekhter A B, Vasilets V N and Fridman A 2008 *Plasma Process. Polym.* **5** 503–33
- [3] Graves D B 2012 *J. Phys. D: Appl. Phys.* **45** 263001
- [4] Samukawa S, Hori M, Rauf S, Tachibana K, Bruggeman P, Kroesen G, Whitehead J C, Murphy A B, Gutsol A F and Starikovskaia S 2012 *J. Phys. D: Appl. Phys.* **45** 253001
- [5] Liu D X, Yang A J, Wang X H, Rong M Z, Iza F and Kong M G 2012 *J. Phys. D: Appl. Phys.* **45** 305205
- [6] Yang A J, Rong M Z, Wang X H, Liu D X and Kong M G 2013 *J. Phys. D: Appl. Phys.* **46** 415201
- [7] Yang A J, Liu D X, Rong M Z, Wang X H and Kong M G 2014 *Phys. Plasmas* **21** 083501
- [8] Dobrynin D, Fridman G, Friedman G and Fridman A 2009 *New J. Phys.* **11** 115020
- [9] Nosenko T, Shimizu T and Morfill G E 2009 *New J. Phys.* **11** 115013
- [10] Xu F, Lu T J and Seffen K A 2008 *J. Mech. Phys. Solids* **56** 1852–84
- [11] Chen C, Liu D X, Liu Z C, Yang A J, Chen H L, Shama G and Kong M G 2014 *Plasma Chem. Plasma Process.* **34** 403–41
- [12] Zhu W D and Lopez J L 2012 *Plasma Sources Sci. Technol.* **21** 034018
- [13] Li H X, Xu T, Chen J M, Zhou H D and Liu H W 2003 *J. Phys. D: Appl. Phys.* **36** 3183
- [14] Chiang M J and Hon M H 2001 *Diam. Relat. Mater.* **10** 1470–6
- [15] Kawamura E, Lieberman M A, Lichtenberg A J and Hudson E A 2007 *J. Vac. Sci. Technol. A* **25** 1456–74
- [16] Kim H J, Kim J Y, Kim J H, Kim D H, Lee D S, Park C S, Park H A, Shin B J and Tae H S 2015 *AIP Adv.* **5** 127141
- [17] Wang J C, Zhang D, Leoni N, Birecki H, Gila O and Kushner M J 2014 *J. Appl. Phys.* **116** 043301
- [18] Yan H, Yang L, Qi X and Ren C 2015 *J. Appl. Phys.* **117** 063302
- [19] Huclova S, Erni D and Fröhlich J 2010 *J. Phys. D: Appl. Phys.* **43** 365405
- [20] Yang A J, Wang X H, Rong M Z, Liu D X, Iza F and Kong M G 2011 *Phys. Plasmas* **18** 113503
- [21] Waskoenig J, Niemi K, Knake N, Graham L M, Reuter S, Schulz-von der Gathen V and Gans T 2010 *Plasma Sources Sci. Technol.* **19** 045018
- [22] Sakiyama Y and Graves D B 2007 *J. Appl. Phys.* **101** 073306
- [23] McKay K, Liu D X, Rong M Z, Iza F and Kong M G 2011 *Appl. Phys. Lett.* **99** 091501
- [24] Vasko C A, Liu D X, Van Veldhuizen E M, Iza F and Bruggeman P J 2014 *Plasma Chem. Plasma Process.* **34** 1081–99
- [25] Walsh J L, Liu D X, Rong M Z and Kong M G 2010 *J. Phys. D: Appl. Phys.* **43** 032001